

The tuberous sclerosis proteins regulate formation of the primary cilium via a rapamycin-insensitive and polycystin 1-independent pathway

Tiffiney R. Hartman¹, Dongyan Liu², Jack T. Zilfou³, Victoria Robb¹, Tasha Morrison¹, Terry Watnick² and Elizabeth P. Henske^{1,4,*}

¹Department of Medical Oncology, Fox Chase Cancer Center, Philadelphia, PA 19090, USA, ²Division of Nephrology, Johns Hopkins School of Medicine, Baltimore, MD 21205, USA, ³Zilfou Therapeutics, Inc, Allentown, PA 18104, USA and ⁴Division of Pulmonary and Critical Care Medicine, Brigham and Women's Hospital, One Blackfan Circle, Karp Building, 6th Floor, Boston, MA 02115, USA

Received July 3, 2008; Revised and Accepted October 7, 2008

Tuberous sclerosis complex (TSC) is a tumor suppressor gene syndrome in which severe renal cystic disease can occur. Many renal cystic diseases, including autosomal dominant polycystic kidney disease (ADPKD), are associated with absence or dysfunction of the primary cilium. We report here that hamartin (TSC1) localizes to the basal body of the primary cilium, and that *Tsc1*^{-/-} and *Tsc2*^{-/-} mouse embryonic fibroblasts (MEFs) are significantly more likely to contain a primary cilium than wild-type controls. In addition, the cilia of *Tsc1*^{-/-} and *Tsc2*^{-/-} MEFs are 17–27% longer than cilia from wild-type MEFs. These data suggest a novel type of ciliary disruption in TSC, associated with enhanced cilia development. The TSC1 and TSC2 proteins function as a heterodimer to inhibit the activity of the mammalian target of rapamycin complex 1 (TORC1). The enhanced ciliary formation in the *Tsc1*^{-/-} and *Tsc2*^{-/-} MEFs was not abrogated by rapamycin, which indicates a TORC1-independent mechanism. Polycystin 1 (PC1), the product of the *PKD1* gene, has been found to interact with TSC2, but *Pkd1*^{-/-} MEFs did not have enhanced ciliary formation. Furthermore, while activation of mTOR has been observed in renal cysts from ADPKD patients, *Pkd1*^{-/-} MEFs did not have evidence of constitutive mTOR activation, thereby underscoring the independent functions of the TSC proteins and PC1 in regulation of primary cilia and mTOR. Our data link the TSC proteins with the primary cilium and reveal a novel phenotype of enhanced ciliary formation in a cyst-associated disease.

INTRODUCTION

Tuberous sclerosis complex (TSC) is a tumor suppressor gene syndrome (1) associated with renal cystic disease (2–7). TSC patients can also develop seizures, mental retardation, autism and tumors in the brain, retina, kidney, heart and skin (8). In a study of 224 TSC patients (74% of whom were under the age of 15), the incidence of renal cysts was 16% in patients with germline *TSC1* mutations and 25% in patients with germline *TSC2* mutations (9). The protein products of the *TSC1* and *TSC2* genes, hamartin and tuberlin, respectively, physically interact (10,11) and function as a heterodimeric complex to

inhibit the mammalian target of rapamycin complex 1 (mTORC1) (12–17). mTORC1 contains mTOR, GβL and Raptor, and controls protein synthesis and cell growth by integrating mitogenic signals and nutrient availability with protein synthesis, via substrates including p70 S6 Kinase (S6K) (18–22). Tuberlin inhibits mTORC1 via the Ras homologue Rheb, which is a key target of tuberlin's highly conserved GTPase activating protein domain (23–28).

Autosomal dominant polycystic kidney disease (ADPKD) is one of the most common hereditary disorders in humans, with a prevalence of about 1:1000 (29). Eighty-five percent of ADPKD is caused by germline mutations in the chromosome

*To whom correspondence should be addressed. Tel: +1 6177755722; Fax: +1 6177327421; Email: ehenske@partners.org

16p13 *PKD1* gene, which encodes the polycystin 1 (PC1) protein, with most of the remaining cases caused by mutations in the chromosome 4q *PKD2* gene, which encodes for polycystin 2 (PC2). Cyst number and size increase with age, eventually numbering in the hundreds or thousands, often leading to dialysis-dependent end-stage renal disease (29). Extra-renal manifestations of ADPKD include cysts in the liver and pancreas, mitral valve prolapse and intracranial and aortic aneurysms (29–31).

TSC2 and *PKD1* are adjacent genes on chromosome 16p13.3, separated by fewer than 100 base pairs. Adults with TSC marked by severe renal cystic disease tend to have large *TSC2* deletions, some of which extend into the 3' end of *PKD1* (2). Contiguous germline deletion of the *TSC2* and *PKD1* genes is associated with severe infantile-onset polycystic kidney disease (2,3,32,33). It was recently reported that tuberlin co-immunoprecipitates with the C-terminal cytoplasmic domain of PC1, and that cysts from patients with ADPKD have evidence of mTOR pathway activation (34), leading to the hypothesis that PC1 inhibits the mTOR pathway via a direct interaction with *TSC2* (35–37).

Many proteins associated with renal cystic disease, including PC1, have been linked with the function of the primary cilium (38–40). It is hypothesized that ciliary-mediated sensation of the environment outside of the cell maintains a growth-arrested phenotype in mature tubules and that loss of ciliary-mediated sensation leads to dysregulated growth (reviewed in 41–50). Proteins associated with ADPKD (PC1, PC2), autosomal recessive PKD (fibrocystin, polaris, cystin, inversion), nephronophthisis (nephrocystin, inversion), oro-facio-digital syndrome (OFD1) and Bardet–Biedl syndrome (BBS proteins 1, 4, 5 and 8) localize to the shaft of the primary cilium, the basal body and/or the centrosome (38,39,42,51–53). The von Hippel–Lindau (VHL) tumor suppressor protein, which is associated with renal cell carcinoma, has also recently been found to localize to the cilium (54,55) and to regulate cilia formation and maintenance (54–56). Mutations in some cyst-associated proteins, including PC1 and PC2, cause defects in the function of the primary cilium (38,46). Mutations in other proteins, including polaris, KIF3A and VHL, lead to shortening or complete loss of the cilium (40,55,57–59), while mutations in the proteins Bbs4 and Nek8 lead to longer cilia (60,61).

The centrosome, composed of two centrioles, serves as the microtubule-organizing center of the cell and regulates cell division, migration and polarity (41). In cells with a primary cilium, the mother centriole of the centrosome serves as the basal body and nucleates cilia development. Several cyst-associated proteins localize to the basal body of the cilium, including BBS-8 (62), nephrocystin-4 (52) and polaris (51). In previous work, we found that endogenous hamartin localizes to the centrosome (63). Here we show that hamartin (TSC1) localizes to the basal body of the primary cilium, and that *Tsc1*^{-/-} and *Tsc2*^{-/-} mouse embryonic fibroblasts (MEFs) have a higher fraction of ciliated cells than control MEFs. In addition, the cilia of *Tsc1*^{-/-} and *Tsc2*^{-/-} MEFs are 17–27% longer than wild-type MEF cilia. This enhanced cilia development was not abrogated by rapamycin, and *Pkd1*^{-/-} MEFs did not have enhanced ciliary formation, indicating that the phenotype

is rapamycin-insensitive and PC1-independent. Despite the previously observed links between *Pkd1* and mTOR, we observe hyperphosphorylation of S6 in only a subset (30–35%) of ADPKD cysts, while the remaining 65–70% have low levels of mTOR activation, suggesting that additional mechanisms are required to fully activate mTOR in human ADPKD or that mTOR is active primarily in early stage disease. In addition, no evidence of mTOR activation was observed in *Pkd1*-null MEFs. Together, these data link the TSC proteins with the primary cilium, suggest a novel paradigm of ciliary signaling disruption in TSC associated with enhanced cilia development, and highlight the independent functions of *TSC2* and PC1 in regulation of the primary cilium and mTOR.

RESULTS

Hamartin (TSC1) is localized to the basal body

We previously reported that TSC1 localizes to the centrosome in Cos7 and HeLa cells (63). Because the centrosome gives rise to the basal body of the primary cilium, we hypothesized that hamartin is basal body localized. Human retinal pigmented epithelial cells (RPE1) were serum starved for 48 h to induce cilia growth, fixed, and co-stained with anti- α -acetylated tubulin antibody to identify cilia, anti- γ -tubulin antibody to identify centrosomes, and anti-hamartin antibody. Endogenous hamartin localized to cytoplasmic vesicular structures as previously reported (10,11) and also to the centrosome in RPE1 cells (arrowheads, Fig. 1A). In cells with a primary cilium, hamartin is localized in the basal body at the base of the cilia (arrows, Fig. 1B). Hamartin also localized to the basal body in a human kidney epithelial cell line, HK-2 (Fig. 1C). To verify the specificity of the hamartin antibody, *Tsc1*-null MEFs (*Tsc1*^{-/-}/vector) and *Tsc1*^{-/-} MEFs with re-introduced TSC1 (*Tsc1*^{-/-}/TSC1) were co-stained with anti- γ -tubulin antibody to identify centrosomes, anti- α -acetylated tubulin antibody to identify cilia, and anti-hamartin antibody. Hamartin colocalized with the centrosome and basal body in the *Tsc1*^{-/-}/TSC1 cells, and not in the *Tsc1*^{-/-}/vector cells (Supplementary Material, Fig. S1A–D).

Loss of hamartin (Tsc1) enhances ciliary formation

The primary cilium is formed and resorbed in connection with the cell cycle, with cilia formation directly after mitosis and cilia disassembly either at cell cycle entry after G₀ or prior to mitotic entry, depending on the cell type (64,65). To determine whether TSC1 regulates ciliary formation, cilia were induced in *Tsc1*^{-/-} and *Tsc1*^{+/+} MEFs by culturing the cells for 48 h after reaching cell contact-induced growth arrest (referred to in subsequent experiments as confluency-induced ciliary formation). Cells were then fixed, probed with antibodies to α -acetylated tubulin (to identify cilia) and γ -tubulin (to identify centrosomes) and scored for cilia by an observer blinded to the experimental conditions. We found that 26% of *Tsc1*^{-/-} MEFs contained a primary cilium, compared with only 5% of *Tsc1*^{+/+} MEFs ($P < 0.005$, Fig. 2A–D). To confirm that this enhanced ciliary formation in the *Tsc1*^{-/-} MEFs was Tsc1-dependent, we examined *Tsc1*^{-/-} MEFs in which either

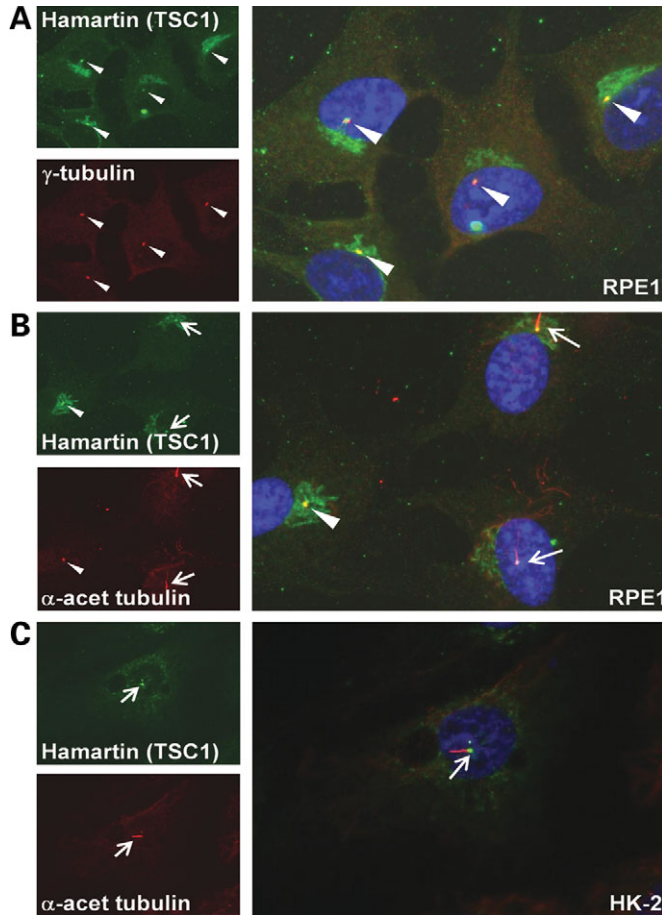


Figure 1. Hamartin localizes to the basal body of ciliated human RPE1 and HK-2 cells. RPE1 and HK-2 cells were serum starved for 48 h to induce cilia formation. (A) RPE1 cells were fixed and immunostained with anti- γ -tubulin antibody (red) to identify centrosomes, and anti-hamartin antibody (TSC1, green). Arrowheads indicate hamartin localization at the centrosome. (B) RPE1 cells were fixed and immunostained with anti- α -acetylated tubulin antibody (red) to identify cilia, and anti-hamartin antibody (TSC1, green). Arrows indicate hamartin at the base of the primary cilia, and arrowheads indicate hamartin in the centrosome of cells lacking a primary cilium. (C) HK-2 cells were fixed and immunostained with anti- α -acetylated tubulin antibody (red) to identify cilia, and anti-hamartin antibody (TSC1, green). Arrow indicates hamartin at the base of the primary cilium. Nuclei were stained with DAPI. All images shown at $\times 100$ magnification.

TSC1 or empty vector was stably re-expressed. A similar trend was observed: 34% of Tsc1-null MEFs (*Tsc1*^{-/-}/vector) contained a primary cilium compared with 12% of *Tsc1*^{-/-} MEFs with re-introduced TSC1 (*Tsc1*^{-/-}/TSC1) ($P < 0.005$, Fig. 2E and F). To confirm further this unexpected finding that loss of Tsc1 enhances ciliary formation, we analyzed cilia at an earlier time point (24 h after plating) during logarithmic growth at subconfluent levels. Twenty percent of the Tsc1-null MEFs had a primary cilium, compared with only 4% of the MEFs re-expressing TSC1 ($P < 0.005$, Fig. 2G). These data indicate that loss of Tsc1 enhances ciliary formation.

In previous work from our laboratory, increased centrosome numbers were observed in Tsc1-null cells during prolonged G1/S arrest (63). To determine whether the Tsc1-null and

Tsc2-null cells have an increased number of centrosomes under the conditions we used to study ciliary formation in this study, we scored cells for centrosomes after 24 or 48 h of growth in full serum or 48 h serum starvation. No differences in centrosome number were detected between *Tsc1*^{-/-}/vector cells (1.1–4.9% of cells with >2 centrosomes, depending on the culture conditions) and *Tsc1*^{-/-}/TSC1 cells (1.2–4% of cells with >2 centrosomes, depending on the culture conditions) (Supplementary Material, Table S1).

Finally, to determine if loss of Tsc1 causes a difference in cilia length, possibly suggesting defects in normal ciliogenesis, we measured the length of *Tsc1*^{-/-}/vector and *Tsc1*^{-/-}/TSC1 cilia after 24 or 48 h in 10% fetal bovine serum (FBS) or 48 h of serum starvation. Interestingly, loss of Tsc1 lead to a 20–27% increase in cilia length, with an average cilia length of 1.54 μm for *Tsc1*^{-/-}/vector cells and 1.18 μm for *Tsc1*^{-/-}/TSC1 cells ($P < 0.005$, Table 1).

Loss of tuberin (Tsc2) enhances ciliary formation

Tuberin and hamartin function as a heterodimer (10,11) and patients with either *TSC1* or *TSC2* mutations can develop renal cysts (1,2). To determine if the enhanced cilia formation we observed in cells lacking hamartin also occurs after loss of tuberin, we analyzed ciliary formation in *Tsc2*^{-/-}*p53*^{-/-} and *Tsc2*^{+/+}*p53*^{-/-} MEFs. These cells, which were originally generated from littermate embryos, are widely used in the TSC field because *Tsc2*^{-/-} MEFs undergo premature senescence and cannot be propagated (66). The *Tsc2*^{-/-}*p53*^{-/-} MEFs had a similar phenotype to the *Tsc1*^{-/-} cells: when ciliary formation was induced by confluency, 70% of the *Tsc2*^{-/-}*p53*^{-/-} MEFs contained a primary cilium compared with only 12% of the *Tsc2*^{+/+}*p53*^{-/-} cells (Fig. 3A–D, $P < 0.005$). When grown for 24 h at subconfluent levels, 43% of the *Tsc2*^{-/-}*p53*^{-/-} MEFs contained a primary cilium compared with only 2% of the *Tsc2*^{+/+}*p53*^{-/-} MEFs ($P < 0.005$, Fig. 3E). To confirm the specificity of this phenotype, we re-expressed GFP-tagged TSC2 in the *Tsc2*^{-/-}*p53*^{-/-} MEFs. Transfected cells were grown for 24 h in 10% FBS, were probed with antibodies to α -acetylated tubulin (to identify cilia) and γ -tubulin (to identify centrosomes), and GFP-TSC2-positive cells (green) and GFP-TSC2-negative cells were scored for cilia. Re-expression of TSC2 reduced the number of ciliated cells from 58 to 12% ($P < 0.005$, Supplementary Material, Fig. S2A–D). Similar to the Tsc1 cells, we found no significant difference in centrosome number between *Tsc2*^{-/-}*p53*^{-/-} (1.3–2.4% of cells with >2 centrosomes, depending on the culture conditions) and *Tsc2*^{+/+}*p53*^{-/-} cells (1.8–3.5% of cells with >2 centrosomes) after 24 or 48 h in 10% FBS, or 48 h serum starvation (Supplementary Material, Table S1).

To determine if loss of Tsc2 is associated with longer cilia, as was observed in the Tsc1-null cells, we measured the length of *Tsc2*^{-/-}*p53*^{-/-} and *Tsc2*^{+/+}*p53*^{-/-} cilia after 24 or 48 h in 10% FBS or 48 h of serum starvation. Loss of Tsc2 lead to a 17–22% increase in cilia length, with an average cilia length of 1.40 μm for *Tsc2*^{-/-}*p53*^{-/-} cells, and 1.13 μm for *Tsc2*^{+/+}*p53*^{-/-} cells ($P < 0.005$, Table 1).

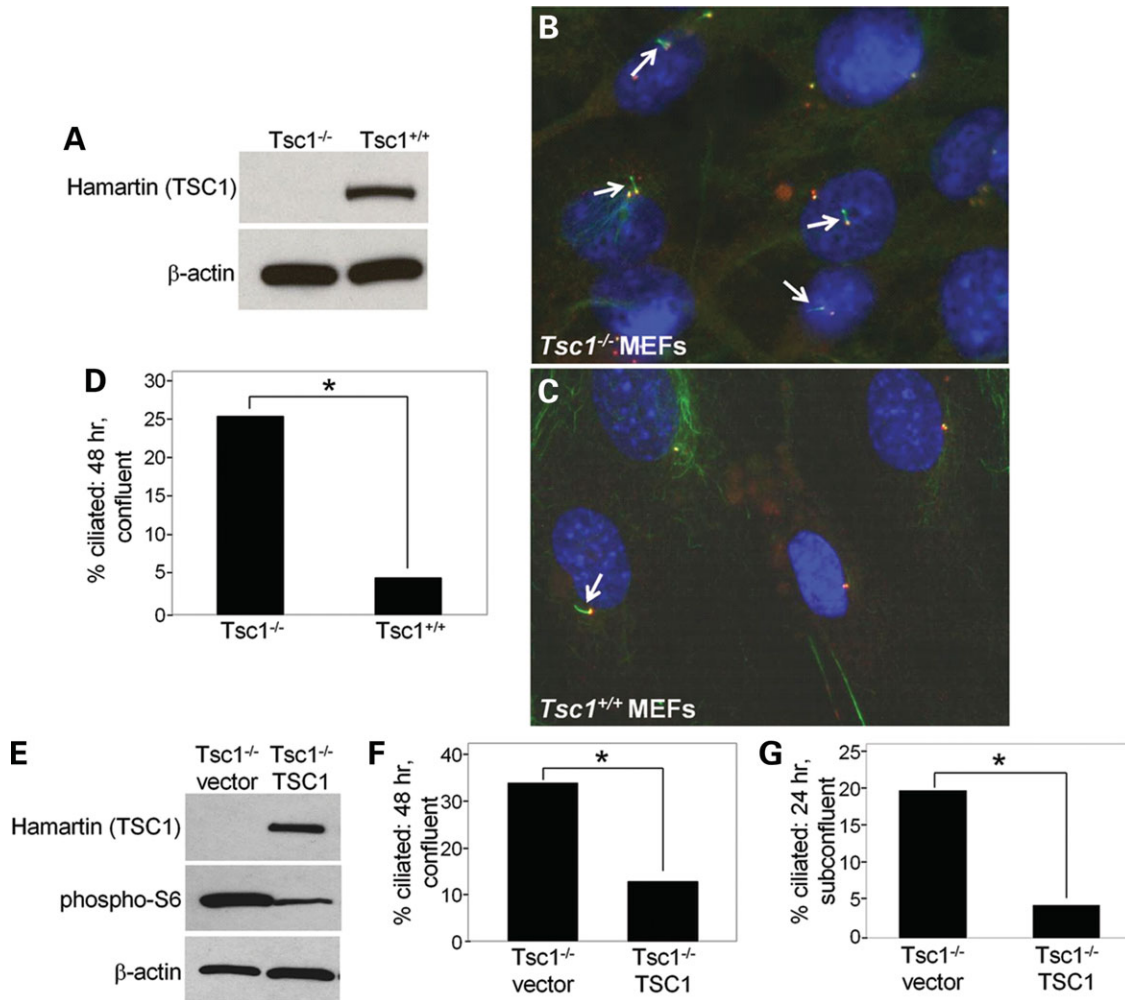


Figure 2. Loss of hamartin (*Tsc1*) enhances ciliary formation. (A) Western immunoblot of *Tsc1^{-/-}* and *Tsc1^{+/+}* cells showing hamartin levels with β -actin as a loading control. (B and C) MEFs were maintained at confluency for 48 h to induce cilia formation. Cells were fixed and immunostained with anti- α -acetylated tubulin antibody (cilia, green) and anti- γ -tubulin antibody (centrosomes/basal body, red). Nuclei were stained with DAPI. Arrows indicate the primary cilia. $\times 100$ magnification. (D) Percentage of cells containing a primary cilium is shown, asterisk indicates $P < 0.005$. (E) Western immunoblot of *Tsc1^{-/-}* cells re-introducing hamartin (*Tsc1*) showing hamartin levels with β -actin as a loading control. Phospho-S6 levels are decreased in cells expressing hamartin, as expected. (F) MEFs were maintained at confluency for 48 h to induce cilia formation. Percentage of cells containing a primary cilium is shown, asterisk indicates $P < 0.005$. (G) Cells were grown in full serum at subconfluent levels for 24 h. Percentage of cells containing a primary cilium is shown, asterisk indicates $P < 0.005$.

Regulation of ciliary formation by *Tsc1* and *Tsc2* is rapamycin-insensitive

The best understood function of TSC1 and TSC2 is to inhibit the activity of mTORC1 (12–15). To determine if the enhancement of cilia formation observed in MEFs lacking TSC proteins is mTORC1-dependent, we treated the cells with the mTORC1 inhibitor, rapamycin. First we analyzed the response to rapamycin in cells in which cilia were induced by confluency. *Tsc1^{-/-}*/vector and *Tsc1^{-/-}*/*TSC1* cells were grown for 48 h in the presence of rapamycin (20 nmol) or dimethyl sulfoxide (DMSO) control. Rapamycin did not abrogate the enhanced cilia development phenotype. In fact, in the *Tsc1^{-/-}*/vector MEFs, rapamycin further increased the number of cells with a primary cilium, from 34% (DMSO) to 52% (rapamycin) ($P < 0.005$, Fig. 4A). To verify that the mTOR pathway remained sensitive to rapamycin after 48 h

growth in 10% FBS, we analyzed phospho-S6 levels by western blot. Phospho-S6 levels were undetectable in *Tsc1^{-/-}*/vector and *Tsc1^{-/-}*/*TSC1* cells treated with rapamycin for 48 h (Supplementary Material, Fig. S3A). No differences in centrosome number were detected in rapamycin-treated cells (Supplementary Material, Table S1), but cilia length was significantly reduced after rapamycin treatment in the *Tsc1^{-/-}*/vector cells, from 1.58 to 1.30 μ m ($P < 0.005$, Table 1).

We also tested the effects of rapamycin on confluency-induced ciliary formation in *Tsc2^{-/-}*/*p53^{-/-}* and *Tsc2^{+/+}*/*p53^{-/-}* MEFs. As in the *Tsc1^{-/-}* cells, rapamycin did not abrogate, but instead enhanced, the cilia development phenotype from 53% (DMSO) to 79% (rapamycin) in *Tsc2^{-/-}*/*p53^{-/-}* cells ($P < 0.005$, Fig. 4B). Similarly, when cilia were induced in the *Tsc2^{-/-}*/*p53^{-/-}* and *Tsc2^{+/+}*/*p53^{-/-}* MEFs by serum deprivation (72 h),

Table 1. Cilia length in *Tsc1* and *Tsc2*-null and wild-type cells

Cell type	Condition	Cilia length, μm average (standard deviation)	Cilia length, μm median	Average cilia length (μm) ^a
<i>Tsc1</i> ^{-/-} /vector	24 h FBS subconfluent	1.48 (± 0.61) ^b	1.4	1.54
	48 h FBS confluency	1.58 (± 0.38) ^b	1.6	
	48 h serum deprivation	1.55 (± 0.43) ^b	1.5	
	48 h FBS, rapamycin	1.30 (± 0.25) ^c	1.3	
<i>Tsc1</i> ^{-/-} /TSC1	24 h FBS subconfluent	1.08 (± 0.22)	1.1	1.18
	48 h FBS confluency	1.22 (± 0.37)	1.2	
	48 h serum deprivation	1.24 (± 0.27)	1.2	
	48 h FBS, rapamycin	1.08 (± 0.27)	1.1	
<i>Tsc2</i> ^{-/-} <i>p53</i> ^{-/-}	24 h FBS subconfluent	1.30 (± 0.30) ^b	1.3	1.40
	48 h FBS confluency	1.35 (± 0.24) ^b	1.3	
	48 h serum deprivation	1.55 (± 0.36) ^b	1.4	
	48 h FBS, rapamycin	1.35 (± 0.25)	1.3	
<i>Tsc2</i> ^{+/+} <i>p53</i> ^{-/-}	24 h FBS subconfluent	1.08 (± 0.25)	1.1	1.13
	48 h FBS confluency	1.11 (± 0.22)	1.1	
	48 h serum deprivation	1.21 (± 0.23)	1.2	
	48 h FBS, rapamycin	1.20 (± 0.34)	1.1	

^aAverage cilia length calculated for each cell line from the three culture conditions: 24 h 10% FBS subconfluent, 48 h 10% FBS confluency and 48 h serum deprivation.

^bCilia length of *Tsc1*^{-/-}/vector compared with *Tsc1*^{-/-}/TSC1, and *Tsc2*^{-/-}*p53*^{-/-} compared with *Tsc2*^{+/+}*p53*^{-/-}, was statistically significant ($P < 0.005$) for all conditions tested, Wilcoxon two sample test.

^cCilia length of rapamycin treated *Tsc1*^{-/-}/vector compared with untreated *Tsc1*^{-/-}/vector at 48 h 10% FBS was statistically significant ($P < 0.005$), Wilcoxon two sample test. Rapamycin treatment of the other three cell lines did not cause a significant reduction in cilia length at 48 h 10% FBS.

rapamycin increased the number of ciliated *Tsc2*^{-/-}*p53*^{-/-} cells from 66% (DMSO) to 76% (≤ 0.05 , Fig. 4C), and increased the number of ciliated *Tsc2*^{+/+}*p53*^{-/-} cells from 32% (DMSO) to 43% ($P < 0.05$). Phospho-S6 levels were undetectable in both *Tsc2*^{-/-}*p53*^{-/-} and *Tsc2*^{+/+}*p53*^{-/-} MEFs treated with rapamycin for 48 or 72 h, confirming the efficacy of rapamycin in these conditions (Supplementary Material, Fig. S3B and C). No differences in centrosome number were detected in rapamycin-treated *Tsc2*^{-/-}*p53*^{-/-} or *Tsc2*^{+/+}*p53*^{-/-} cells (Supplementary Material, Table S1). Unlike the *Tsc1* cells, rapamycin treatment had no effect on cilia length in the *Tsc2*^{-/-}*p53*^{-/-} and *Tsc2*^{+/+}*p53*^{-/-} MEFs, which indicates the possibility of a role of p53 in ciliary length regulation (Table 1).

Interestingly, when the *Tsc2*^{-/-}*p53*^{-/-} MEFs were serum starved for 72 h to induce cilia, 9% had multiple cilia per cell (range 2–11 cilia/cell, average 3 cilia/cell), when compared with <1% of *Tsc2*^{+/+}*p53*^{-/-} MEFs ($P < 0.005$, Fig. 4D–G). This phenotype was rapamycin-sensitive, with 3.7% of the rapamycin-treated *Tsc2*^{-/-}*p53*^{-/-} MEFs having more than 1 cilia ($P < 0.05$, Fig. 4D). Taken together, these data indicate that loss of *Tsc2* leads to two ciliary phenotypes: enhanced ciliary formation, which is rapamycin-insensitive, and multiple cilia per cell, which is rapamycin-sensitive.

Regulation of ciliary formation by *Tsc2* is independent of PC1

PC1 has been shown to bind to TSC2, and it is hypothesized that cells lacking PC1 have functional inactivation of TSC2 leading to mTOR activation (34–37). Based on this model, we predicted that cells lacking PC1 would have enhanced ciliary formation similarly to cells lacking TSC2. To test this, we utilized MEFs derived from embryos with homozygous disruption of exons 2 and 3 of *Pkd1* (67,68). These

Pkd1^{-/-} mice have an embryonic lethal phenotype associated with severely cystic kidneys. First, to determine whether MEFs normally express PC1 at a level analogous to those of renal epithelial cells, we used quantitative real-time RT-PCR to compare *Pkd1* mRNA levels in *Pkd1*^{+/+} and *Pkd1*^{-/-} MEFs with IMCD3 (inner medullary collecting duct) cells, which are frequently used to study PC1 function, and with mPKE (non-immortalized mouse primary kidney epithelial) cells. *Pkd1*^{+/+} MEFs actually had a higher *Pkd1* mRNA level (relative level 100) than IMCD3 and mPKE cells (relative level 12 and 13, respectively), while the *Pkd1*^{-/-} MEFs had nearly undetectable *Pkd1* levels (Fig. 5A). Next, to directly compare the *Pkd1*^{-/-} MEFs to *Tsc2*^{-/-}*p53*^{-/-} MEFs with a similar genetic background, early passage *Pkd1*^{+/+} and *Pkd1*^{-/-} MEFs were retrovirally transduced with p53 shRNA to generate immortalized *Pkd1*^{+/+}*p53kd*(knockdown) and *Pkd1*^{-/-}*p53kd* MEFs (69). These cells have a >97% decrease in p53 levels as determined by quantitative real-time RT-PCR (Fig. 5B). Finally, to determine if *Pkd1*^{-/-}*p53kd* cells have enhanced cilia development similar to *Tsc2*^{-/-}*p53*^{-/-} MEFs, cells were grown at subconfluent levels in full serum media for 24 h, fixed, stained and scored for the presence of cilia. As we had observed in previous experiments, the *Tsc2*^{-/-}*p53*^{-/-} MEFs had a markedly elevated number of ciliated cells, compared with the *Tsc2*^{+/+}*p53*^{-/-} MEFs (43 versus 2%, $P < 0.005$). In striking contrast to *Tsc2*^{-/-}*p53*^{-/-} MEFs, only 8% of the *Pkd1*^{-/-}*p53kd* MEFs had a primary cilium ($P < 0.005$, Fig. 5C). These data demonstrate that TSC1 and TSC2 function primarily independently of PC1 to regulate primary cilium development in fibroblasts. The fact that *Pkd1*^{-/-}*p53kd* MEFs had a small, but statistically higher number of cells with a cilium compared with *Tsc2*^{+/+}*p53*^{-/-} MEFs, leaves open the possibility that PC1 may have a minor effect on cilia formation.

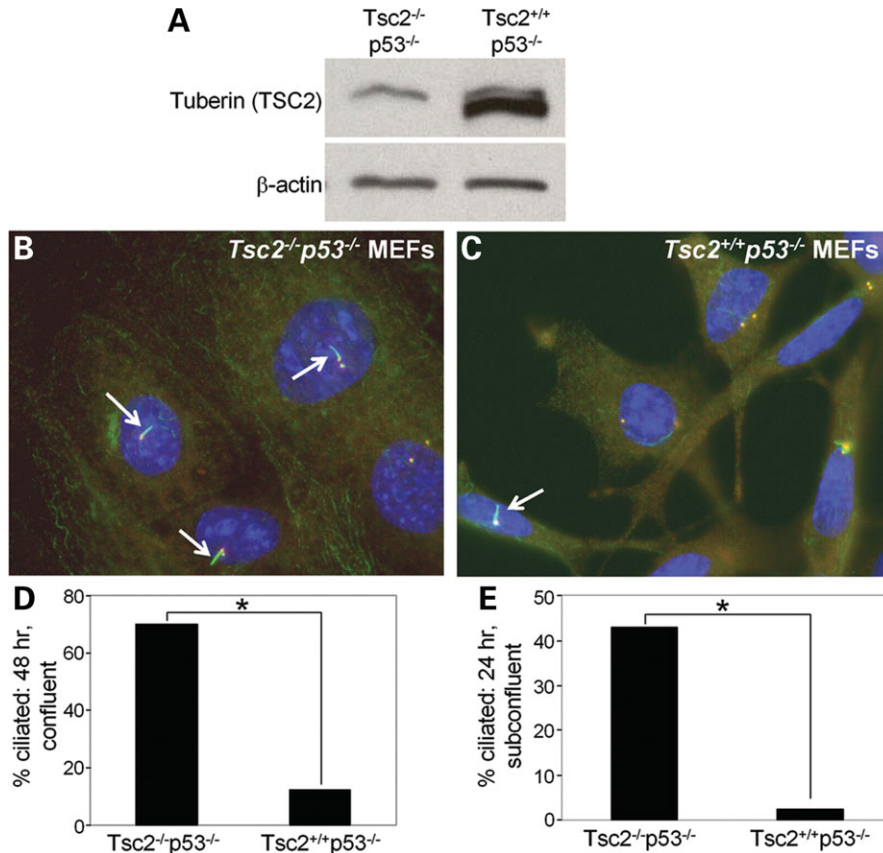


Figure 3. Loss of tuberlin (*Tsc2*) enhances ciliary formation. (A) Western immunoblot of *Tsc2*^{-/-}*p53*^{-/-} and *Tsc2*^{+/+}*p53*^{-/-} cells showing tuberlin levels with β-actin as a loading control. The upper band appearing in both lanes is a cross-reactive band often observed with this antibody. (B and C) *Tsc2*^{-/-}*p53*^{-/-} MEFs and *Tsc2*^{+/+}*p53*^{-/-} MEFs were maintained at confluency for 48 h to induce cilia formation. Cells were fixed and immunostained with anti-α-acetylated tubulin antibody (cilia, green) and anti-γ-tubulin antibody (centrosomes/basal body, red). Nuclei were stained with DAPI. Arrows indicate the primary cilia. ×100 magnification. (D) Percentage of cells containing a primary cilium is shown, asterisk indicates $P < 0.005$. (E) Cells were grown in full serum at subconfluent levels for 24 h. Percentage of cells containing a primary cilium is shown, asterisk indicates $P < 0.005$.

Loss of *Pkd1* does not constitutively activate the mTOR pathway in fibroblasts

The fact that cells lacking PC1 and cells lacking *Tsc2* have different phenotypes related to ciliary formation led us to examine mTOR activation in the *Pkd1*-null cells. To our knowledge, no prior study has addressed whether PC1-null cells have dysregulation of the mTOR pathway. To examine the role of *Pkd1* in mTOR regulation, we compared *Pkd1*^{-/-}*p53kd* MEFs to *Pkd1*^{+/+}*p53kd* and *Tsc2*^{-/-}*p53*^{-/-} MEFs. After 24 h of serum deprivation, the *Tsc2*^{-/-}*p53*^{-/-} MEFs had high levels of phosphorylated ribosomal protein S6 (phospho-S6) as expected because of the known role of TSC2 in inhibiting mTOR. In contrast, both the *Pkd1*^{+/+}*p53kd* and *Pkd1*^{-/-}*p53kd* MEFs had low levels of phospho-S6 after 24 h of serum deprivation. Fifteen minutes after serum stimulation, both the *Pkd1*^{+/+}*p53kd* and the *Pkd1*^{-/-}*p53kd* MEFs showed marked enhancement of mTOR activation (Fig. 6A). To confirm that this effect is related to the loss of *Pkd1*, and not a consequence of p53 loss, we compared early passage primary cultures of *Pkd1*^{-/-} MEFs to the *Pkd1*^{-/-}*p53kd* MEFs and *Tsc2*^{-/-}*p53*^{-/-} MEFs. Both primary and immortalized *Pkd1*^{-/-} MEFs had low levels of phospho-S6 in serum

deprivation conditions (Fig. 6B). These data demonstrate that loss of PC1 does not constitutively activate mTOR in fibroblasts.

ADPKD kidneys contain cysts both with and without evidence of mTOR activation

Because cells lacking PC1 have low levels of activated mTOR in serum deprivation conditions, we next re-examined mTOR activation in ADPKD. Paraffin-embedded tissue specimens from 7 ADPKD patients were stained with anti-phospho-S6 ribosomal protein (Ser 235/236), and 121 individual cysts were scored using a semi-quantitative scale as reported previously (70,71). Strong (3+) to moderate (2+) phospho-S6 immunoreactivity was evident in 36 cysts (30%) (Table 2). Importantly, the other 70% had weak (1+) or negative phospho-S6 immunoreactivity. Similar staining patterns were observed using anti-phospho-mTOR (Ser2448), with 35% of cysts staining strongly or moderately positive (Table 3). Both positively staining and negatively staining cysts were identified in each patient, as illustrated in Figure 7. Cysts tended to have a homogeneous staining pattern, with the entire cyst staining either positive or negative. Weakly

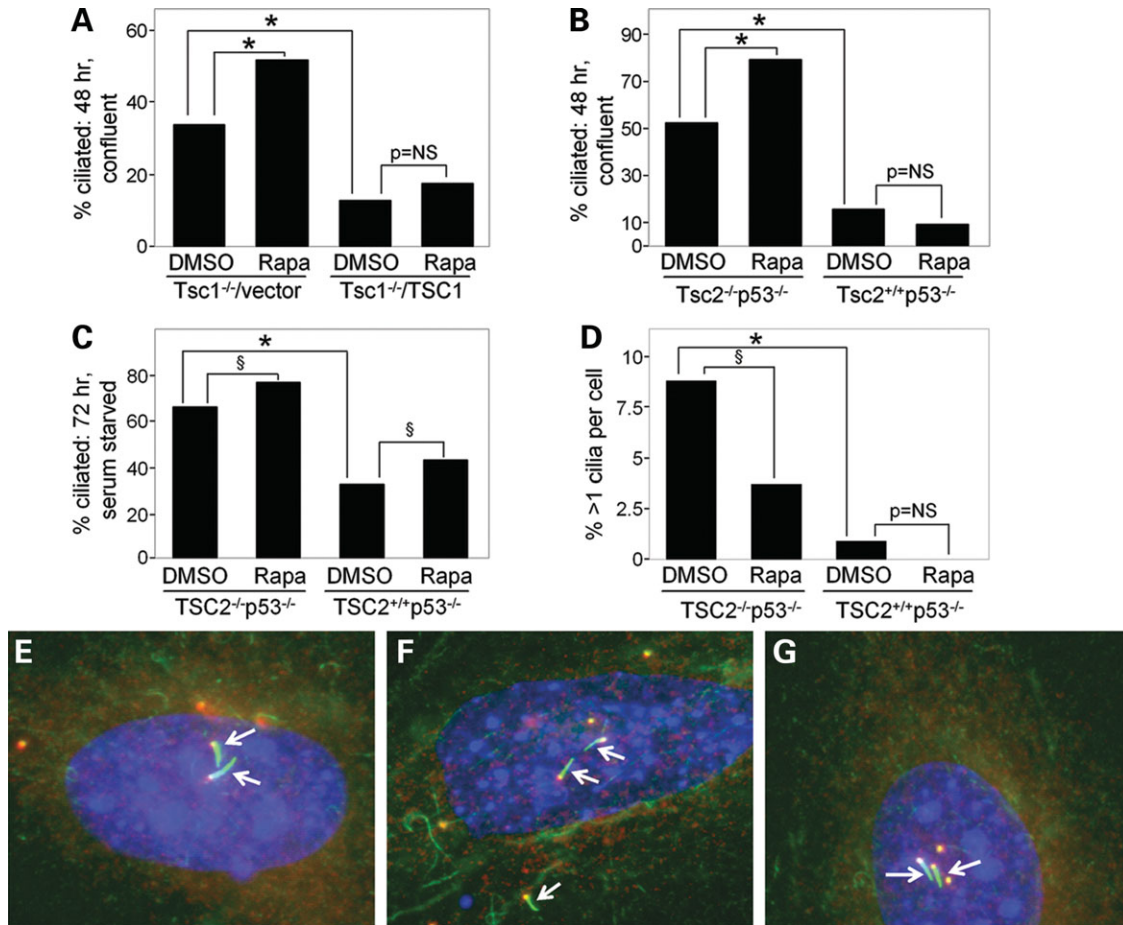


Figure 4. Regulation of ciliary formation by *Tsc1* and *Tsc2* is rapamycin-insensitive. (A) *Tsc1*^{-/-}/vector and *Tsc1*^{-/-}/TSC1 MEFs were grown in the presence of 10% FBS for 48 h with rapamycin (20 nmol) or DMSO control. Percentage of cells containing a primary cilium is shown, asterisk indicates $P < 0.005$, $P = \text{NS}$, no significant difference. (B) *Tsc2*^{-/-}p53^{-/-} and *Tsc2*^{+/+}p53^{-/-} MEFs were grown in the presence of 10% FBS for 48 h with rapamycin (20 nmol) or DMSO control. Percentage of cells containing a primary cilium is shown, asterisk indicates $P < 0.005$, $P = \text{NS}$, no significant difference. (C and D) *Tsc2*^{-/-}p53^{-/-} and *Tsc2*^{+/+}p53^{-/-} MEFs were serum starved for 72 h in the presence of rapamycin (20 nmol) or DMSO control. (C) Percentage of cells containing a primary cilium is shown. (D) Percentage of cells containing more than one primary cilium is shown, asterisk indicates $P < 0.005$, section sign indicates $P < 0.05$, $P = \text{NS}$, no significant difference. (E–G) Examples are shown of single *Tsc2*^{-/-}p53^{-/-} cells containing more than one primary cilium. MEFs were serum starved for 72 h, fixed and immunostained with anti- α -acetylated tubulin antibody (cilia, green) and anti- γ -tubulin antibody (centrosomes/basal body, red). Nuclei were stained with DAPI. Arrows indicate primary cilia. $\times 100$ magnification.

positive phosphorylation of S6 was seen in the renal epithelium of some normal renal tubules (not shown), as we have previously observed (70). In some cases, the phospho-S6 and phospho-mTOR-positive cells were larger and more cuboidal in shape than the negative cells (arrows, Fig. 7).

The fact that only $\sim 30\%$ of ADPKD cysts have evidence of activation of the mTOR/S6K signaling pathway was unexpected, for this implies that mutational inactivation of *PKD1* is not sufficient to activate mTOR. One possible explanation for the discordance between these results and the hypothesized PC1-TSC2-TOR signaling axis (which would predict uniform activation of mTOR in *PKD1* cysts) is that mTOR is initially uniformly active, but that fibrosis and consequent hypoxia in end-stage disease inhibit mTOR.

DISCUSSION

The mechanisms through which mutations in the *TSC1* or *TSC2* genes contribute to the development of renal cysts are

not well understood. We report here that TSC1 is localized to the basal body of the primary cilium, and that fibroblasts lacking either *Tsc1* or *Tsc2* have a phenotype of enhanced ciliary formation in three different conditions: logarithmic growth; confluency-induced ciliary formation and serum deprivation-induced growth arrest. In addition, cells lacking *Tsc1* or *Tsc2* have cilia that are on average 17–27% longer than wild-type cells, which indicates a defect in normal ciliogenesis. The pathogenesis of many renal cystic diseases has been linked with dysfunction of the primary cilium (e.g. ADPKD, autosomal recessive PKD, nephronophthisis, OFD1 and BBS; 42–44,50,52,53,72). Mutations in some proteins associated with renal cystic disease result in complete loss of the primary cilium (e.g. polaris, KIF3A and VHL) (51,55,57–59), while increases in ciliary length have been reported in cell culture and kidney tubules from mutations in the renal cystic disease associated Bbs4 and Nek8 proteins (60,61). To our knowledge, increased ciliary formation has not been previously observed in cells carrying mutations for

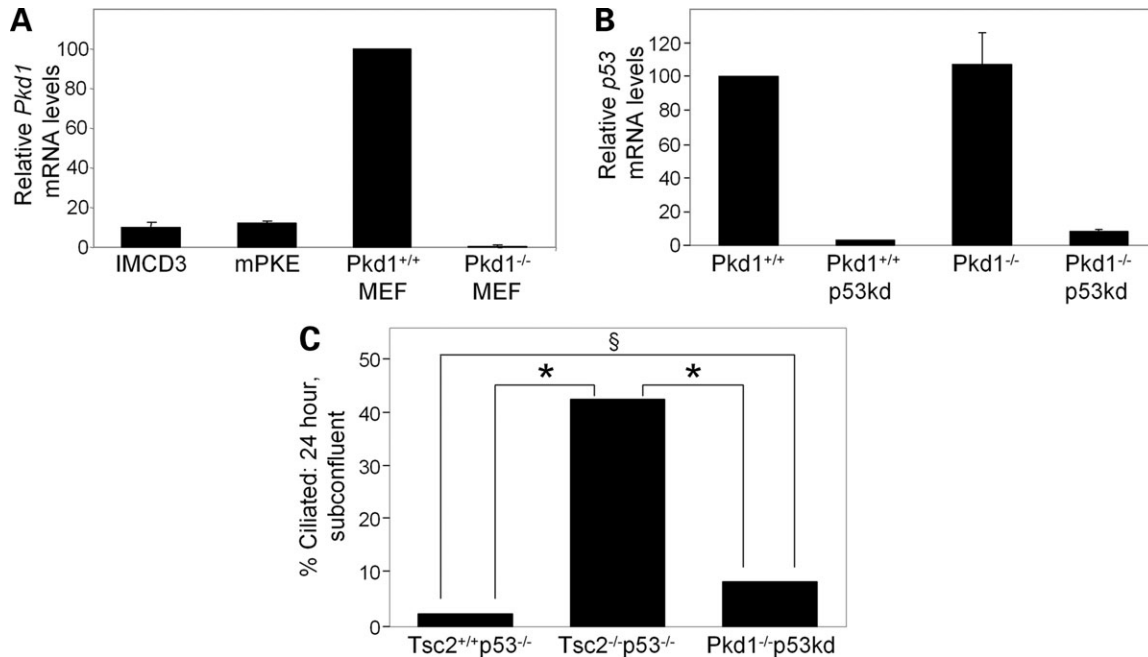


Figure 5. *Pkd1*^{-/-} *p53kd* cells do not have enhanced cilia development. (A) Quantitative real-time RT-PCR analysis of *Pkd1* mRNA levels in IMCD3 cells, non-immortalized mouse primary kidney epithelial (mPKE) cells, *Pkd1*^{+/+} MEFs and *Pkd1*^{-/-} MEFs. RNA concentration was determined by Nanodrop spectrophotometry, and RT-PCR results are normalized to levels of TATA-binding protein. (B) Quantitative real-time RT-PCR analysis of p53 levels of *Pkd1*^{+/+} and *Pkd1*^{-/-} MEFs before and after immortalization with p53 shRNA. (C) Cells were grown in full serum at subconfluency for 24 h. Percentage of cells containing a primary cilium is shown, asterisk indicates $P < 0.005$, section sign indicates $P < 0.05$.

genes associated with renal cystic disease. These data, therefore, may reveal a novel paradigm in which enhanced ciliary development is associated with renal cyst pathogenesis.

The best studied function of the TSC1 and TSC2 proteins is to inhibit the activity of mTORC1 (12–17,23–28). We found that *Tsc1*^{-/-} and *Tsc2*^{-/-} *p53*^{-/-} MEFs treated with the mTORC1 inhibitor rapamycin actually increased, rather than reduced cilia numbers, which demonstrates that the enhanced cilia formation in these cells is mTORC1-independent. The relative contributions of mTOR-dependent and mTOR-independent mechanisms to cyst pathogenesis in TSC are not known. In a *Tsc1*^{+/-} mouse model, only 53 and 37% of cyst epithelial cells were positive for phospho-mTOR and phospho-S6 immunostaining, respectively, compared with >90% of cystadenomas and renal cell carcinomas that stained positively for both markers. This suggests that activation of the mTOR pathway may not be the key initiating event in cyst development (73). It is known that treatment with rapamycin reduces the size of renal angiomyolipomas in patients with TSC (74) and reduces the severity of kidney lesions (cysts and tumors) in rodent models (75–77), but the impact of rapamycin on cystic disease in humans with TSC is not yet known. Our unexpected finding that rapamycin treatment further enhances cilia formation in the *Tsc1* and *Tsc2*-null cells may have important implications for treating renal cystic disease in TSC patients. This may suggest that the TSC proteins regulate the primary cilium through both mTORC1-dependent and mTORC1-independent mechanisms. These mechanisms may differentially impact ciliary assembly, elongation and/or maintenance, and in turn these mechanisms may differentially impact cyst initiation and

cyst progression. The efficacy of rapamycin on renal cystic disease in patients carrying TSC gene mutations or a contiguous *PKD1/TSC2* deletion may therefore differ from the efficacy of rapamycin on renal cystic disease in patients carrying *PKD1* mutations.

In addition to enhanced ciliary formation, 9% of *Tsc2*^{-/-} *p53*^{-/-} MEFs had multiple primary cilia per cell, which was partially corrected by treatment with rapamycin. Therefore, the TSC pathway appears to have both mTOR-independent and mTOR-dependent roles in ciliary formation. We have previously observed that *Tsc1*^{-/-} MEFs have extra centrosomes after a 40 h G₁/S arrest (63), and others have reported that *Tsc2*^{+/*EK*} pulmonary vascular smooth muscle cells (SMCs) derived from Eker rats have increased centrosome number compared with *Tsc2*^{+/*+*} SMCs (78). However, under the conditions used to study ciliary formation in this study, extra centrosomes were not observed in either the *Tsc1*-null or the *Tsc2*-null cells, which suggests that the multiple-cilia-per-cell phenotype is not a consequence of multiple centrosomes (63).

Mutations in either *TSC1* or *TSC2* alone can lead to polycystic kidney disease, but renal failure is uncommon. Mutations in *PKD1* alone lead to renal failure in 50% of cases, at an average age of 60 years (29,30). The severe renal cystic disease observed in infants with contiguous deletion of both *TSC2* and *PKD1* is consistent with a synergistic functional connection between TSC and ADPKD (2,3,32,79). It has been previously shown that TSC2 is required for correct localization of PC1 to the cell membrane, placing TSC2 upstream of PC1 (80). More recently, it has been proposed that PC1 inhibits the activity of mTOR via a direct interaction

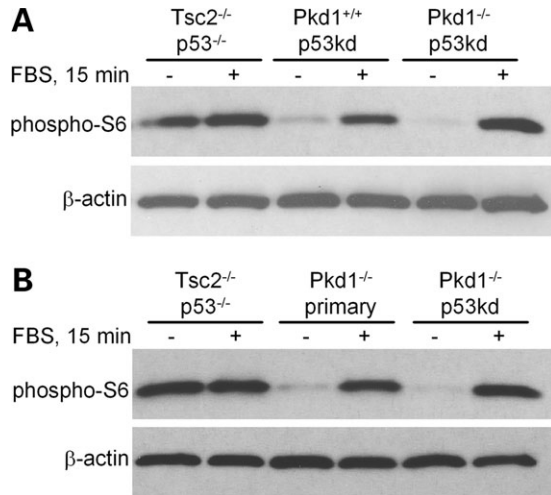


Figure 6. Loss of *Pkd1* does not constitutively activate the mTOR pathway. MEFs were serum deprived overnight, then stimulated for 15 min in the presence of 20% FBS. Immunoblots were probed with phospho-S6 to determine the level of mTOR activation. β -actin was used as a loading control. (A) Western immunoblot of *Tsc2*^{-/-}*p53*^{-/-}, *Pkd1*^{+/+}*p53kd* MEFs and *Pkd1*^{-/-}*p53kd* MEFs. (B) Western immunoblot of *Tsc2*^{-/-}*p53*^{-/-}, *Pkd1*^{-/-} primary MEFs and *Pkd1*^{-/-}*p53kd* MEFs. Similar results were seen in four independent experiments.

with TSC2, placing PC1 upstream of TSC2 (34). We found that *Pkd1*^{-/-} MEFs do not exhibit enhanced cilia development as do the *Tsc1*^{-/-} and *Tsc2*^{-/-}*p53*^{-/-} MEFs, indicating that at least for this particular ciliary phenotype, PC1 is not functioning upstream of TSC2. PC1 localizes to the primary cilium and is involved in sensing physiological fluid flow (38,39,81,82). We speculate, therefore, that TSC2 and PC1 may cooperatively regulate different aspects of ciliary development and function, with TSC2 regulating ciliary formation and PC1 sensing physiological fluid flow, thereby synergistically contributing to renal cyst formation in patients with contiguous deletion of both genes.

In striking contrast to *Tsc2*^{-/-}*p53*^{-/-} MEFs, *Pkd1*^{-/-} MEFs showed no evidence of mTOR activation under serum deprivation conditions. This is surprising considering the interaction of PC1 (overexpressed C-terminal cytoplasmic tail) with TSC2 that was hypothesized to underlie the activation of mTOR observed in renal cystic epithelial cells from patients with ADPKD (34–37). One possible explanation is that the *Pkd1* disruption in the *Pkd1*^{-/-} MEFs used for our studies, which occurs by homologous recombination of a β -galactosidase/neomycin cassette in place of exons 2 and 3 of *Pkd1*, leaves a partially functional region of PC1 intact (67,68). A second potential explanation for the discordance between our data and the previously proposed models for the relationship between PC1 and TSC2 is that there are differences in the regulation of mTOR activity by PC1 between fibroblasts and epithelial cells. This could be clinically important since ADPKD patients develop non-epithelial manifestations, including mitral valve prolapse and aortic and intracranial aneurysms (29–31,83). However, we note that MEFs have been used by other groups to study the roles of VHL, PDGFR α , KIF3A and other proteins in ciliary formation and function, and in general, results have

Table 2. Phospho-S6 immunoreactivity of ADPKD renal cysts

Patient number	Number of cysts scored			
	-	1+	2+	3+
305	6	7	3	1
427	2	4	1	0
433	11	10	5	3
513	6	1	3	1
550	3	3	1	0
555	16	6	2	6
611	8	2	7	3
Total number (%)	52 (43)	33 (27)	22 (18)	14 (12)

Anti-phospho-S6 ribosomal protein (Ser 235/236) staining of cyst lining epithelial cells was scored using a semi-quantitative scale of negative (-), weakly positive (1+), moderately positive (2+) or strongly positive (3+), as reported previously (70,71).

been concordant between fibroblasts and epithelial cells when both cell types were analyzed (55,84–87).

Multiple signaling cascades converge on TSC2, leading to its phosphorylation and inactivation (88–92). Interestingly, loss of *Pkd1* has been shown to result in activation of Akt and MAPK (93,94), and Akt and MAPK activation can lead to mTOR activation via direct phosphorylation and inactivation of TSC2 (88–91), yet mTOR was not activated in our *Pkd1*^{-/-} MEFs. While loss of PC1 does not appear sufficient to activate mTORC1, it may act cooperatively with other pathways to potentiate cyst pathogenesis (Fig. 8). Consistent with this, we find that ~30–35% of ADPKD cysts have strong to moderate immunohistochemical evidence of mTOR pathway activation, while 65–70% do not, potentially reflecting activation of other pathways upstream of TSC2 and mTOR.

Elucidating the mechanism through which mTOR is regulated in ADPKD has critical clinical implications, since at least four clinical trials of mTOR inhibitors are ongoing for patients with PKD to determine if these drugs can slow cyst progression, reduce cyst volume and improve renal function (95). Our data suggest that mutational activation of *PKD1* is not sufficient to activate mTOR and that other events which may be mediated by TSC2 are required to activate mTOR in ADPKD cysts, thereby leading to cyst progression. These other events may distinguish cyst initiation from cyst progression and could reveal novel therapeutic options for patients with ADPKD, which affects 12.5 million people world-wide, accounts for 8–10% of all patients on dialysis, and leads to \$2 billion per year in health care costs in the USA.

MATERIALS AND METHODS

Cell culture

Human retinal pigmented epithelial cells (hTERT-RPE1) were obtained from the American Type Culture Collection. RPE1 cells were maintained in 1:1 DMEM:F12 media containing 10% FBS and 10 μ g/ml Hygromycin B. Immortalized human kidney proximal tubule epithelial (HK-2) cells (American Type Culture Collection) were maintained in DMEM with 10% FBS and ITS liquid media supplement (Sigma). *Tsc1*^{+/+}, *Tsc1*^{-/-}, *Tsc2*^{+/+}*p53*^{-/-}, and *Tsc2*^{-/-}*p53*^{-/-} MEFs have been previously described (6,66,96) and were

Table 3. Phospho-mTOR immunoreactivity of ADPKD renal cysts

Patient number	Number of cysts scored			
	-	1+	2+	3+
305	20	6	5	10
427	23	4	6	7
Total number (%)	43 (53)	10 (12)	11 (14)	17 (21)

Anti-phospho-mTOR (Ser 2448) staining of cyst lining epithelial cells was scored using a semi-quantitative scale of negative (-), weakly positive (1+), moderately positive (2+) or strongly positive (3+), as reported previously (70,71).

maintained in DMEM with 10% FBS and non-essential amino acids. TSC1-null re-introduction MEFs have been previously described (63). Non-immortalized mPKE were derived from a wild-type C57BL/6 mouse and were maintained in low calcium DMEM/F12 media (Invitrogen #90-5212EF) with 5% horse serum. The *Pkd1*^{-/-} MEFs were isolated from *Pkd1*^{-/-} mice that have homologous recombination of a β -galactosidase/neomycin cassette that disrupts exons 2 and 3 (67,68). Wild-type and *Pkd1*^{-/-} MEFs were immortalized by transduction of a retroviral vector containing shRNA targeting p53 (69). For immortalization, 5×10^6 293T Phoenix packaging cells were transfected with 7 μ g shRNA plasmid (p53E or empty vector) with 5 μ g helper plasmid containing retroviral *gag/pol* genes using Fugene 6 (Roche). After 48 h, the target MEFs were infected twice daily for 2 days with the media from the Phoenix cells filtered through a 0.45 μ m filter. MEF media was changed twice daily for the next 2 days, and then media was supplemented with 1.5 μ g puromycin to select for infected cells for the next 72 h. All cells losing p53 are immortalized, and puromycin selection is no longer necessary.

Assays of ciliary formation

To study cilia three different conditions were used, as specified in the text: cells were serum starved for 48–72 h to induce cilia formation, cells were cultured with cell-to-cell contact inhibition in the presence of 10% FBS for 48 h to induce ciliary formation, or cells were grown logarithmically in the presence of 10% FBS at subconfluency for 24 h. Each result was confirmed in at least three independent experiments. Due to variation in seeding density, absolute numbers of primary cilia differed between experiments by 10–30%, but the fold increase caused by loss of *Tsc1* or *Tsc2* remained consistent. Rapamycin (20 nmol) and DMSO were added to the media for the full 48 or 72 h of ciliary induction, as indicated. For GFP-TSC2 re-expression in *Tsc2*^{-/-}*p53*^{-/-} MEFs, cells were plated on coverslips and transfected with GFP-TSC2 plasmid DNA using Fugene 6 (Roche). After 24 h growth in 10% FBS, cells were fixed and stained. For each culture condition, at least 150 cells were scored for the presence of a primary cilium, and at least 200 cells scored for the number of centrosomes by an observer blinded to the experimental conditions. For cilia measurements, at least 50 randomly chosen cilia were measured (from base to tip) per cell line for each culture condition at 1000 \times magnification using a Nikon Coolsnap ES camera and Image-Pro Express 2000 software (Media Cybernetics, Inc.).

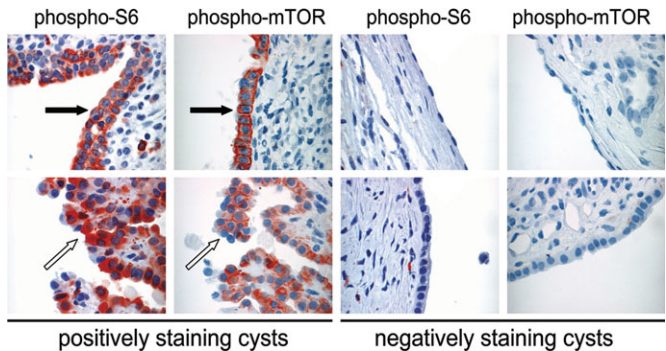


Figure 7. ADPKD kidneys contain cysts both with and without evidence of mTOR activation. Cysts from seven ADPKD patients were stained using phospho-S6 (Ser 235/236) and phospho-mTOR (Ser 2448) antibodies. Thirty percent had moderate or strong immunoreactivity with anti-phospho-S6, and 35% had moderate or strong immunoreactivity with anti-phospho-mTOR. Representative examples of positive and negative cysts are shown. Phospho-mTOR and phospho-S6-positive cysts tended to have larger cells with a more cuboidal shape (black arrow). The negative cells tended to have a flattened shape. Occasionally, the phospho-S6 and phospho-mTOR-positive cysts had papillary projections (white arrows, patient 611). $\times 40$ magnification.

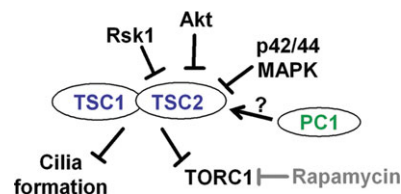


Figure 8. Working model. TSC1 and TSC2 regulate cilia formation in a TORC1/rapamycin-independent manner. Multiple signaling cascades, including MAPK, Akt and Rsk1, converge on TSC2, leading to its phosphorylation and inactivation and contributing to mTOR activation. Loss of PC1 does not appear sufficient to activate TOR or impact ciliary formation via TSC2. However, PC1 may cooperate with the multiple signaling cascades to initiate or enhance cystogenesis.

Immunofluorescence

RPE1, HK-2 or MEF cells were grown in conditions to stimulate cilia formation and then fixed for 10 min in 100% methanol on ice. Cells were washed three times in PBS, incubated for 5 min in 0.2% Triton-X in PBS, and then washed three times in Triton-X PBS. Primary antibodies [α -acetylated tubulin (Sigma) 1:1000, γ -tubulin (Abcam) 1:1000, Hamartin (Zymed) 1:100] were added for 1 h at room temperature, and then cells were washed three times with Triton-PBS. Secondary antibody [alexa fluor 488 or 594 (Molecular Probes) 1:1000] were added for 1 h at room temperature, then cells were washed 3 \times 2 min with Triton-PBS. Cells were incubated with DAPI for 1 min at room temperature, washed in PBS and mounted using anti-fading gel mount (Biomedica). Cells were viewed by Nikon Coolsnap ES and pictures taken with Image-Pro Express 2000 software (Media Cybernetics).

Western blotting

Cells were washed once in PBS on ice, then lysed in PTY buffer (50 mM HEPES, pH 7.5, 50 mM NaCl, 50 mM NaF,

10 mM Na₄P₂O₇·10H₂O, 5 mM EDTA, 1% Triton X, Sigma protease inhibitors), or in RIPA buffer (150 mM NaCl, 50 mM Tris, pH 8.0, 1% Triton X, 1% deoxycholic acid, 0.1% SDS, 2 mM PMSF, Sigma protease inhibitors). Proteins were run on 4–20% SDS–PAGE, then transferred to Immobilon-P (Millipore) membrane. Western blots were probed with antibodies to β-actin (Sigma, A2228), hamartin [TSC1] (Zymed, 37–0400), phospho-S6 ribosomal protein [Ser235/236] (Cell Signaling, 2211) and tuberlin [TSC2] (Santa Cruz, sc-893).

Immunohistochemistry

ADPKD specimens were obtained at the time of nephrectomy through the Polycystic Kidney Research Foundation. Formalin-fixed, paraffin-embedded ADPKD kidney sections were deparaffinized and rehydrated according to standard procedures. Slides were boiled in 10 mM citrate buffer, pH 6.0 for 10 min in the microwave. After cooling, slides were quenched with 3% hydrogen peroxide in methanol for 30 min at room temperature. For staining procedures, the Histo-stain Plus kit (Zymed) was used according to manufacturer's instructions. Phospho-S6 [(Ser235/236) Cell Signaling] and phospho-mTOR [(Ser2448) #2967] antibodies were used in a 1:50 dilution in PBS. Cysts were scored for phospho-S6 and phospho-mTOR staining using a scale of negative (–), weakly positive (1+), moderately positive (2+) or strongly positive (3+).

Reverse transcription polymerase chain reaction

Total mRNA was isolated from IMCD3, mPKE and MEF cell lines using the RNeasyTM Mini-kit (Qiagen). RNA concentration was determined using NanoDropTM Spectrophotometer (Thermo Scientific). For each sample, two reverse transcription reactions were performed with 100 and 20 ng of input RNA. 5'-Nuclease assays using TaqMan chemistry were run on a 7900 HT sequence detection system (Applied Biosystems). Ct (cycle threshold) values were converted to quantities (in arbitrary units) using standard curve (five points, 5-fold dilutions) established with a calibrator sample. Quantitative real-time RT–PCR results were normalized to TATA-binding protein mRNA levels. For each sample, the two values of relative quantity (from two PCR assays) were averaged.

Statistical analysis

A two-tailed Fisher's exact test was used for all statistical analysis of cilia number per cell and centrosome number per cell. For comparisons of cilia length, a Wilcoxon two sample test was performed. Significance was achieved at $P \leq 0.05$.

SUPPLEMENTARY MATERIAL

Supplementary Material is available at HMG Online.

ACKNOWLEDGEMENTS

We thank Erica Golemis for critical reading of this manuscript. We thank Dr Sam Litwin and Tianyu Li at the Fox Chase Cancer Center Biostatistics Facility for statistical analysis. We thank Emmanuelle Nicolas for assistance with quantitative real-time RT–PCR. We thank Olga Plotnikova for mPKE cells.

Conflict of Interest statement. None declared.

FUNDING

This work was supported by grants from the PKD Foundation and Tuberous Sclerosis Alliance (#-01PT07a). T.R.H. was supported by NIH F32 (DK076443-01). Funding to pay the Open Access charges was provided by Brigham and Women's Hospital.

REFERENCES

- Gomez, M.R., Sampson, J.R. and Whittemore, V.H. (1999) *Tuberous Sclerosis Complex*, Oxford University Press, New York.
- Sampson, J.R., Maheshwar, M.M., Aspinwall, R., Thompson, P., Cheadle, J.P., Ravine, D., Roy, S., Haan, E., Bernstein, J. and Harris, P.C. (1997) Renal cystic disease in tuberous sclerosis: role of the polycystic kidney disease 1 gene. *Am. J. Hum. Genet.*, **61**, 843–851.
- Longa, L., Scolari, F., Brusco, A., Carbonara, C., Polidoro, S., Valzorio, B., Riegler, P., Migone, N. and Maiorca, R. (1997) A large TSC2 and PKD1 gene deletion is associated with renal and extrarenal signs of autosomal dominant polycystic kidney disease. *Nephrol. Dial. Transplant.*, **12**, 1900–1907.
- Kobayashi, T., Hirayama, Y., Kobayashi, E., Kubo, Y. and Hino, O. (1995) A germline insertion in the tuberous sclerosis (Tsc2) gene gives rise to the Eker rat model of dominantly inherited cancer. *Nat. Genet.*, **9**, 70–74.
- Kobayashi, T., Minowa, O., Kuno, J., Mitani, H., Hino, O. and Noda, T. (1999) Renal carcinogenesis, hepatic hemangiomas, and embryonic lethality caused by a germ-line Tsc2 mutation in mice. *Cancer Res.*, **59**, 1206–1211.
- Onda, H., Lueck, A., Marks, P.W., Warren, H.B. and Kwiatkowski, D.J. (1999) Tsc2(+/-) mice develop tumors in multiple sites that express gelsoin and are influenced by genetic background. *J. Clin. Invest.*, **104**, 687–695.
- Kobayashi, T., Minowa, O., Sugitani, Y., Takai, S., Mitani, H., Kobayashi, E., Noda, T. and Hino, O. (2001) A germ-line Tsc1 mutation causes tumor development and embryonic lethality that are similar, but not identical to, those caused by Tsc2 mutation in mice. *Proc. Natl Acad. Sci. USA*, **98**, 8762–8767.
- Shepherd, C.W., Gomez, M.R., Lie, J.T. and Crowson, C.S. (1991) Causes of death in patients with tuberous sclerosis. *Mayo Clin. Proc.*, **66**, 792–796.
- Dabora, S.L., Jozwiak, S., Franz, D.N., Roberts, P.S., Nieto, A., Chung, J., Choy, Y.S., Reeve, M.P., Thiele, E., Egelhoff, J.C. *et al.* (2001) Mutational analysis in a cohort of 224 tuberous sclerosis patients indicates increased severity of TSC2, compared with TSC1, disease in multiple organs. *Am. J. Hum. Genet.*, **68**, 64–80.
- Plank, T.L., Yeung, R.S. and Henske, E.P. (1998) Hamartin, the product of the tuberous sclerosis 1 (TSC1) gene, interacts with tuberlin and appears to be localized to cytoplasmic vesicles. *Cancer Res.*, **58**, 4766–4770.
- van Slegtenhorst, M., Nellist, M., Nagelkerken, B., Cheadle, J., Snell, R., van den Ouweland, A., Reuser, A., Sampson, J., Halley, D. and van der Sluijs, P. (1998) Interaction between hamartin and tuberlin, the TSC1 and TSC2 gene products. *Hum. Mol. Genet.*, **7**, 1053–1057.
- Radimerski, T., Montagne, J., Hemmings-Mieszczak, M. and Thomas, G. (2002) Lethality of *Drosophila* lacking TSC tumor suppressor function rescued by reducing dS6K signaling. *Genes Dev.*, **16**, 2627–2632.
- Inoki, K., Li, Y., Zhu, T., Wu, J. and Guan, K.L. (2002) TSC2 is phosphorylated and inhibited by Akt and suppresses mTOR signalling. *Nat. Cell Biol.*, **4**, 648–657.

14. Gao, X., Zhang, Y., Arrazola, P., Hino, O., Kobayashi, T., Yeung, R.S., Ru, B. and Pan, D. (2002) Tsc tumour suppressor proteins antagonize amino-acid-TOR signalling. *Nat. Cell Biol.*, **4**, 699–704.
15. Potter, C.J., Huang, H. and Xu, T. (2001) *Drosophila* Tsc1 functions with Tsc2 to antagonize insulin signaling in regulating cell growth, cell proliferation, and organ size. *Cell*, **105**, 357–368.
16. Jaeschke, A., Hartkamp, J., Saitoh, M., Roworth, W., Nobukuni, T., Hodges, A., Sampson, J., Thomas, G. and Lamb, R. (2002) Tuberous sclerosis complex tumor suppressor-mediated S6 kinase inhibition by phosphatidylinositol-3-OH kinase is mTOR independent. *J. Cell Biol.*, **159**, 217–224.
17. Tapon, N., Ito, N., Dickson, B.J., Treisman, J.E. and Hariharan, I.K. (2001) The *Drosophila* tuberous sclerosis complex gene homologs restrict cell growth and cell proliferation. *Cell*, **105**, 345–355.
18. Kim, D.H., Sarbassov, D.D., Ali, S.M., King, J.E., Latek, R.R., Erdjument-Bromage, H., Tempst, P. and Sabatini, D.M. (2002) mTOR interacts with raptor to form a nutrient-sensitive complex that signals to the cell growth machinery. *Cell*, **110**, 163–175.
19. Kozma, S.C. and Thomas, G. (2002) Regulation of cell size in growth, development and human disease: PI3K, PKB and S6K. *Bioessays*, **24**, 65–71.
20. Blume-Jensen, P. and Hunter, T. (2001) Oncogenic kinase signalling. *Nature*, **411**, 355–365.
21. Shah, O.J., Anthony, J.C., Kimball, S.R. and Jefferson, L.S. (2000) 4E-BP1 and S6K1: translational integration sites for nutritional and hormonal information in muscle. *Am. J. Physiol. Endocrinol. Metab.*, **279**, E715–E729.
22. Loewith, R., Jacinto, E., Wullschlegel, S., Lorberg, A., Crespo, J.L., Bonenfant, D., Oppliger, W., Jenoe, P. and Hall, M.N. (2002) Two TOR complexes, only one of which is rapamycin sensitive, have distinct roles in cell growth control. *Mol. Cell*, **10**, 457–468.
23. Zhang, Y., Gao, X., Saucedo, L.J., Ru, B., Edgar, B.A. and Pan, D. (2003) Rheb is a direct target of the tuberous sclerosis tumour suppressor proteins. *Nat. Cell Biol.*, **5**, 578–581.
24. Garami, A., Zwartkruis, F.J., Nobukuni, T., Joaquin, M., Roccio, M., Stocker, H., Kozma, S.C., Hafen, E., Bos, J.L. and Thomas, G. (2003) Insulin activation of Rheb, a mediator of mTOR/S6K/4E-BP signaling, is inhibited by TSC1 and 2. *Mol. Cell*, **11**, 1457–1466.
25. Inoki, K., Li, Y., Xu, T. and Guan, K.L. (2003) Rheb GTPase is a direct target of TSC2 GAP activity and regulates mTOR signaling. *Genes Dev.*, **17**, 1829–1834.
26. Saucedo, L.J., Gao, X., Chiarelli, D.A., Li, L., Pan, D. and Edgar, B.A. (2003) Rheb promotes cell growth as a component of the insulin/TOR signalling network. *Nat. Cell Biol.*, **5**, 566–571.
27. Tee, A.R., Manning, B.D., Roux, P.P., Cantley, L.C. and Blenis, J. (2003) Tuberous sclerosis complex gene products, Tuberin and Hamartin, control mTOR signaling by acting as a GTPase-activating protein complex toward Rheb. *Curr. Biol.*, **13**, 1259–1268.
28. Stocker, H., Radimerski, T., Schindelholz, B., Wittwer, F., Belawat, P., Daram, P., Breuer, S., Thomas, G. and Hafen, E. (2003) Rheb is an essential regulator of S6K in controlling cell growth in *Drosophila*. *Nat. Cell Biol.*, **5**, 559–565.
29. Wilson, P.D. (2004) Polycystic kidney disease. *N. Engl. J. Med.*, **350**, 151–164.
30. Gabow, P.A. (1993) Autosomal dominant polycystic kidney disease. *N. Engl. J. Med.*, **329**, 332–342.
31. Chapman, A.B., Rubinstein, D., Hughes, R., Stears, J.C., Earnest, M.P., Johnson, A.M., Gabow, P.A. and Kaehny, W.D. (1992) Intracranial aneurysms in autosomal dominant polycystic kidney disease. *N. Engl. J. Med.*, **327**, 916–920.
32. Brook-Carter, P.T., Peral, B., Ward, C.J., Thompson, P., Hughes, J., Maheshwar, M.M., Nellist, M., Gamble, V., Harris, P.C. and Sampson, J.R. (1994) Deletion of the TSC2 and PKD1 genes associated with severe infantile polycystic kidney disease—a contiguous gene syndrome. *Nat. Genet.*, **8**, 328–332.
33. Ong, A.C., Harris, P.C., Davies, D.R., Pritchard, L., Rossetti, S., Biddolph, S., Vaux, D.J., Migone, N. and Ward, C.J. (1999) Polycystin-1 expression in PKD1, early-onset PKD1, and TSC2/PKD1 cystic tissue. *Kidney Int.*, **56**, 1324–1333.
34. Shillingford, J.M., Murcia, N.S., Larson, C.H., Low, S.H., Hedgepeth, R., Brown, N., Flask, C.A., Novick, A.C., Goldfarb, D.A., Kramer-Zucker, A. *et al.* (2006) From the Cover: The mTOR pathway is regulated by polycystin-1, and its inhibition reverses renal cystogenesis in polycystic kidney disease. *Proc. Natl Acad. Sci. USA*, **103**, 5466–5471.
35. Mostov, K.E. (2006) mTOR is out of control in polycystic kidney disease. *Proc. Natl Acad. Sci. USA*, **103**, 5247–5248.
36. Weimbs, T. (2006) Regulation of mTOR by polycystin-1: is polycystic kidney disease a case of futile repair? *Cell Cycle*, **5**, 2425–2429.
37. Chapman, A.B. (2007) Autosomal dominant polycystic kidney disease: time for a change? *J. Am. Soc. Nephrol.*, **18**, 1399–1407.
38. Nauli, S.M., Alenghat, F.J., Luo, Y., Williams, E., Vassilev, P., Li, X., Elia, A.E., Lu, W., Brown, E.M., Quinn, S.J. *et al.* (2003) Polycystins 1 and 2 mediate mechanosensation in the primary cilium of kidney cells. *Nat. Genet.*, **33**, 129–137.
39. Yoder, B.K., Hou, X. and Guay-Woodford, L.M. (2002) The polycystic kidney disease proteins, polycystin-1, polycystin-2, polaris, and cystin, are co-localized in renal cilia. *J. Am. Soc. Nephrol.*, **13**, 2508–2516.
40. Yoder, B.K., Tousson, A., Millican, L., Wu, J.H., Bugg, C.E. Jr, Schafer, J.A. and Balkovetz, D.F. (2002) Polaris, a protein disrupted in orpk mutant mice, is required for assembly of renal cilium. *Am. J. Physiol. Renal Physiol.*, **282**, F541–F552.
41. Badano, J.L., Teslovich, T.M. and Katsanis, N. (2005) The centrosome in human genetic disease. *Nat. Rev. Genet.*, **6**, 194–205.
42. Pan, J., Wang, Q. and Snell, W.J. (2005) Cilium-generated signaling and cilia-related disorders. *Lab. Invest.*, **85**, 452–463.
43. Afzelius, B.A. (2004) Cilia-related diseases. *J. Pathol.*, **204**, 470–477.
44. Pazour, G.J. and Rosenbaum, J.L. (2002) Intraflagellar transport and cilia-dependent diseases. *Trends Cell Biol.*, **12**, 551–555.
45. Salisbury, J.L. (2004) Primary cilia: putting sensors together. *Curr. Biol.*, **14**, R765–R767.
46. Nauli, S.M. and Zhou, J. (2004) Polycystins and mechanosensation in renal and nodal cilia. *Bioessays*, **26**, 844–856.
47. Chodhari, R., Mitchison, H.M. and Meeks, M. (2004) Cilia, primary ciliary dyskinesia and molecular genetics. *Paediatr. Respir. Rev.*, **5**, 69–76.
48. Yokoyama, T. (2004) Motor or sensor: a new aspect of primary cilia function. *Anat. Sci. Int.*, **79**, 47–54.
49. Calvet, J.P. (2002) Cilia in PKD—letting it all hang out. *J. Am. Soc. Nephrol.*, **13**, 2614–2616.
50. Lina, F. and Satlin, L.M. (2004) Polycystic kidney disease: the cilium as a common pathway in cystogenesis. *Curr. Opin. Pediatr.*, **16**, 171–176.
51. Taulman, P.D., Haycraft, C.J., Balkovetz, D.F. and Yoder, B.K. (2001) Polaris, a protein involved in left-right axis patterning, localizes to basal bodies and cilia. *Mol. Biol. Cell*, **12**, 589–599.
52. Mollet, G., Silbermann, F., Delous, M., Salomon, R., Antignac, C. and Saunier, S. (2005) Characterization of the nephrocystin/nephrocystin-4 complex and subcellular localization of nephrocystin-4 to primary cilia and centrosomes. *Hum. Mol. Genet.*, **14**, 645–656.
53. Pazour, G.J. (2004) Intraflagellar transport and cilia-dependent renal disease: the ciliary hypothesis of polycystic kidney disease. *J. Am. Soc. Nephrol.*, **15**, 2528–2536.
54. Schermer, B., Ghenoiu, C., Bartram, M., Muller, R.U., Kotsis, F., Hohne, M., Kuhn, W., Rapka, M., Nitschke, R., Zentgraf, H. *et al.* (2006) The von Hippel-Lindau tumor suppressor protein controls ciliogenesis by orienting microtubule growth. *J. Cell Biol.*, **175**, 547–554.
55. Thoma, C.R., Frew, I.J., Hoerner, C.R., Montani, M., Moch, H. and Krek, W. (2007) pVHL and GSK3beta are components of a primary cilium-maintenance signalling network. *Nat. Cell Biol.*, **9**, 588–595.
56. Esteban, M.A., Harten, S.K., Tran, M.G. and Maxwell, P.H. (2006) Formation of primary cilia in the renal epithelium is regulated by the von Hippel-Lindau tumor suppressor protein. *J. Am. Soc. Nephrol.*, **17**, 1801–1806.
57. Lutz, M.S. and Burk, R.D. (2006) Primary cilium formation requires von Hippel-Lindau gene function in renal-derived cells. *Cancer Res.*, **66**, 6903–6907.
58. Pazour, G.J., Dickert, B.L., Vucica, Y., Seeley, E.S., Rosenbaum, J.L., Witman, G.B. and Cole, D.G. (2000) Chlamydomonas IFT88 and its mouse homologue, polycystic kidney disease gene tg737, are required for assembly of cilia and flagella. *J. Cell Biol.*, **151**, 709–718.
59. Lin, F., Hiesberger, T., Cordes, K., Sinclair, A.M., Goldstein, L.S., Somlo, S. and Igarashi, P. (2003) Kidney-specific inactivation of the KIF3A subunit of kinesin-II inhibits renal ciliogenesis and produces polycystic kidney disease. *Proc. Natl Acad. Sci. USA*, **100**, 5286–5291.

60. Mokrzan, E.M., Lewis, J.S. and Mykytyn, K. (2007) Differences in renal tubule primary cilia length in a mouse model of Bardet-Biedl syndrome. *Nephron Exp. Nephrol.*, **106**, e88–e96.
61. Smith, L.A., Bukanov, N.O., Husson, H., Russo, R.J., Barry, T.C., Taylor, A.L., Beier, D.R. and Ibraghimov-Beskrovnaya, O. (2006) Development of polycystic kidney disease in juvenile cystic kidney mice: insights into pathogenesis, ciliary abnormalities, and common features with human disease. *J. Am. Soc. Nephrol.*, **17**, 2821–2831.
62. Ansley, S.J., Badano, J.L., Blacque, O.E., Hill, J., Hoskins, B.E., Leitch, C.C., Kim, J.C., Ross, A.J., Eichers, E.R., Teslovich, T.M. *et al.* (2003) Basal body dysfunction is a likely cause of pleiotropic Bardet-Biedl syndrome. *Nature*, **425**, 628–633.
63. Astrinidis, A., Senapedis, W. and Henske, E.P. (2006) Hamartin, the tuberous sclerosis complex 1 gene product, interacts with polo-like kinase 1 in a phosphorylation-dependent manner. *Hum. Mol. Genet.*, **15**, 287–297.
64. Quarmby, L.M. and Parker, J.D. (2005) Cilia and the cell cycle? *J. Cell Biol.*, **169**, 707–710.
65. Pugacheva, E.N., Jablonski, S.A., Hartman, T.R., Henske, E.P. and Golemis, E.A. (2007) HEF1-dependent Aurora A activation induces disassembly of the primary cilium. *Cell*, **129**, 1351–1363.
66. Zhang, H., Cicchetti, G., Onda, H., Koon, H.B., Asrican, K., Bajraszewski, N., Vazquez, F., Carpenter, C.L. and Kwiatkowski, D.J. (2003) Loss of Tsc1/Tsc2 activates mTOR and disrupts PI3K-Akt signaling through downregulation of PDGFR. *J. Clin. Invest.*, **112**, 1223–1233.
67. Garcia-Gonzalez, M.A., Menezes, L.F., Piontek, K.B., Kaimori, J., Huso, D.L., Watnick, T., Onuchic, L.F., Guay-Woodford, L.M. and Germino, G.G. (2007) Genetic interaction studies link autosomal dominant and recessive polycystic kidney disease in a common pathway. *Hum. Mol. Genet.*, **16**, 1940–1950.
68. Piontek, K.B., Huso, D.L., Grinberg, A., Liu, L., Bedja, D., Zhao, H., Gabrielson, K., Qian, F., Mei, C., Westphal, H. *et al.* (2004) A functional floxed allele of Pkd1 that can be conditionally inactivated in vivo. *J. Am. Soc. Nephrol.*, **15**, 3035–3043.
69. Hemann, M.T., Fridman, J.S., Zilfou, J.T., Hernando, E., Paddison, P.J., Cordon-Cardo, C., Hannon, G.J. and Lowe, S.W. (2003) An epi-allelic series of p53 hypomorphs created by stable RNAi produces distinct tumor phenotypes in vivo. *Nat. Genet.*, **33**, 396–400.
70. Robb, V.A., Karbowiczek, M., Klein-Szanto, A.J. and Henske, E.P. (2007) Activation of the mTOR signaling pathway in renal clear cell carcinoma. *J. Urol.*, **177**, 346–352.
71. Karbowiczek, M., Spittle, C.S., Morrison, T., Wu, H. and Henske, E.P. (2008) mTOR is activated in the majority of malignant melanomas. *J. Invest. Dermatol.*, **128**, 980–987.
72. Nachury, M.V., Loktev, A.V., Zhang, Q., Westlake, C.J., Peranen, J., Merdes, A., Slusarski, D.C., Scheller, R.H., Bazan, J.F., Sheffield, V.C. *et al.* (2007) A core complex of BBS proteins cooperates with the GTPase Rab8 to promote ciliary membrane biogenesis. *Cell*, **129**, 1201–1213.
73. Wilson, C., Bonnet, C., Guy, C., Idziaszczyk, S., Colley, J., Humphreys, V., Maynard, J., Sampson, J.R. and Cheadle, J.P. (2006) Tsc1 haploinsufficiency without mammalian target of rapamycin activation is sufficient for renal cyst formation in Tsc1^{+/-} mice. *Cancer Res.*, **66**, 7934–7938.
74. Davies, D.M., Johnson, S.R., Tattersfield, A.E., Kingswood, J.C., Cox, J.A., McCartney, D.L., Doyle, T., Elmslie, F., Saggarr, A., de Vries, P.J. *et al.* (2008) Sirolimus therapy in tuberous sclerosis or sporadic lymphangioliomyomatosis. *N. Engl. J. Med.*, **358**, 200–203.
75. Messina, M.P., Rauhut, A., Lee, L. and Dabora, S.L. (2007) Tuberous sclerosis preclinical studies: timing of treatment, combination of a rapamycin analog (CCI-779) and interferon-gamma, and comparison of rapamycin to CCI-779. *BMC Pharmacol.*, **7**, 14.
76. Kenerson, H., Dundon, T.A. and Yeung, R.S. (2005) Effects of rapamycin in the Eker rat model of tuberous sclerosis complex. *Pediatr. Res.*, **57**, 67–75.
77. Lee, L., Sudentas, P., Donohue, B., Asrican, K., Worku, A., Walker, V., Sun, Y., Schmidt, K., Albert, M.S., El-Hashemite, N. *et al.* (2005) Efficacy of a rapamycin analog (CCI-779) and IFN-gamma in tuberous sclerosis mouse models. *Genes Chromosomes Cancer*, **42**, 213–227.
78. Gui, Y., He, G.H., Walsh, M.P. and Zheng, X.L. (2007) Predisposition to tetraploidy in pulmonary vascular smooth muscle cells derived from the Eker rats. *Am. J. Physiol. Lung Cell. Mol. Physiol.*, **293**, L702–L711.
79. Martignoni, G., Bonetti, F., Pea, M., Tardanico, R., Brunelli, M. and Eble, J.N. (2002) Renal disease in adults with TSC2/PKD1 contiguous gene syndrome. *Am. J. Surg. Pathol.*, **26**, 198–205.
80. Kleymenova, E., Ibraghimov-Beskrovnaya, O., Kugoh, H., Everitt, J., Xu, H., Kiguchi, K., Landes, G., Harris, P. and Walker, C. (2001) Tuberin-dependent membrane localization of polycystin-1: a functional link between polycystic kidney disease and the TSC2 tumor suppressor gene. *Mol. Cell*, **7**, 823–832.
81. Low, S.H., Vasanth, S., Larson, C.H., Mukherjee, S., Sharma, N., Kinter, M.T., Kane, M.E., Obara, T. and Weimbs, T. (2006) Polycystin-1, STAT6 and P100 function in a pathway that transduces ciliary mechanosensation and is activated in polycystic kidney disease. *Dev. Cell*, **10**, 57–69.
82. Xu, C., Rossetti, S., Jiang, L., Harris, P.C., Brown-Glaberman, U., Wandering-Ness, A., Bacallao, R. and Alper, S.L. (2007) Human ADPKD primary cyst epithelial cells with a novel, single codon deletion in the PKD1 gene exhibit defective ciliary polycystin localization and loss of flow-induced Ca²⁺ signaling. *Am. J. Physiol. Renal Physiol.*, **292**, F930–F945.
83. Huston, J., 3rd, Torres, V.E., Sullivan, P.P., Offord, K.P. and Wiebers, D.O. (1993) Value of magnetic resonance angiography for the detection of intracranial aneurysms in autosomal dominant polycystic kidney disease. *J. Am. Soc. Nephrol.*, **3**, 1871–1877.
84. Schneider, L., Clement, C.A., Teilmann, S.C., Pazour, G.J., Hoffmann, E.K., Satir, P. and Christensen, S.T. (2005) PDGFRalpha signaling is regulated through the primary cilium in fibroblasts. *Curr. Biol.*, **15**, 1861–1866.
85. Shalom, O., Shalva, N., Altschuler, Y. and Motro, B. (2008) The mammalian Nek1 kinase is involved in primary cilium formation. *FEBS Lett.*, **582**, 1465–1470.
86. Tallila, J., Jakkula, E., Peltonen, L., Salonen, R. and Kestila, M. (2008) Identification of CC2D2A as a Meckel syndrome gene adds an important piece to the ciliopathy puzzle. *Am. J. Hum. Genet.*, **82**, 1361–1367.
87. Corbit, K.C., Shyer, A.E., Dowdle, W.E., Gauden, J., Singla, V., Chen, M.H., Chuang, P.T. and Reiter, J.F. (2008) Kif3a constrains beta-catenin-dependent Wnt signalling through dual ciliary and non-ciliary mechanisms. *Nat. Cell Biol.*, **10**, 70–76.
88. Manning, B.D., Tee, A.R., Logsdon, M.N., Blenis, J. and Cantley, L.C. (2002) Identification of the tuberous sclerosis complex-2 tumor suppressor gene product tuberin as a target of the phosphoinositide 3-kinase/akt pathway. *Mol. Cell*, **10**, 151–162.
89. Manning, B.D. and Cantley, L.C. (2003) United at last: the tuberous sclerosis complex gene products connect the phosphoinositide 3-kinase/Akt pathway to mammalian target of rapamycin (mTOR) signalling. *Biochem. Soc. Trans.*, **31**, 573–578.
90. Cai, S.L., Tee, A.R., Short, J.D., Bergeron, J.M., Kim, J., Shen, J., Guo, R., Johnson, C.L., Kiguchi, K. and Walker, C.L. (2006) Activity of TSC2 is inhibited by AKT-mediated phosphorylation and membrane partitioning. *J. Cell Biol.*, **173**, 279–289.
91. Tee, A.R., Anjum, R. and Blenis, J. (2003) Inactivation of the tuberous sclerosis complex-1 and -2 gene products occurs by phosphoinositide 3-kinase/Akt-dependent and -independent phosphorylation of tuberin. *J. Biol. Chem.*, **278**, 37288–37296.
92. Roux, P.P., Ballif, B.A., Anjum, R., Gygi, S.P. and Blenis, J. (2004) Tumor-promoting phorbol esters and activated Ras inactivate the tuberous sclerosis tumor suppressor complex via p90 ribosomal S6 kinase. *Proc. Natl. Acad. Sci. USA*, **101**, 13489–13494.
93. Qian, A.L., Du, H., King, B.F., Kumar, S., Dean, P.G., Cosio, F.G. and Torres, V.E. (2008) Sirolimus reduces polycystic liver volume in ADPKD patients. *J. Am. Soc. Nephrol.*, **19**, 631–638.
94. Shibazaki, S., Yu, Z., Nishio, S., Tian, X., Thomson, R.B., Mitobe, M., Louvi, A., Velazquez, H., Ishibe, S., Cantley, L.G. *et al.* (2008) Cyst formation and activation of the extracellular regulated kinase pathway after kidney specific inactivation of Pkd1. *Hum. Mol. Genet.*, **17**, 1505–1516.
95. Serra, A.L., Kistler, A.D., Poster, D., Strucker, M., Wuthrich, R.P., Weishaupt, D. and Tschirch, F. (2007) Clinical proof-of-concept trial to assess the therapeutic effect of sirolimus in patients with autosomal dominant polycystic kidney disease: SUISSSE ADPKD study. *BMC Nephrol.*, **8**, 13.
96. Kwiatkowski, D.J., Zhang, H., Bandura, J.L., Heiberger, K.M., Glogauer, M., el-Hashemite, N. and Onda, H. (2002) A mouse model of TSC1 reveals sex-dependent lethality from liver hemangiomas, and up-regulation of p70S6 kinase activity in Tsc1 null cells. *Hum. Mol. Genet.*, **11**, 525–534.